

# First-Principles Study of Nanoparticle–Biomolecular Interactions: Anchoring of a (ZnO)<sub>12</sub> Cluster on Nucleobases

Vasundhara Shewale,<sup>†,‡</sup> Prachi Joshi,<sup>†,§</sup> Saikat Mukhopadhyay,<sup>†</sup> Mrinalini Deshpande,<sup>‡</sup> Ravindra Pandey,<sup>\*,†</sup> Saber Hussain,<sup>||</sup> and Shashi P. Karna<sup>\*,⊥</sup>

<sup>†</sup>Department of Physics, Michigan Technological University, Houghton, Michigan 49931, United States

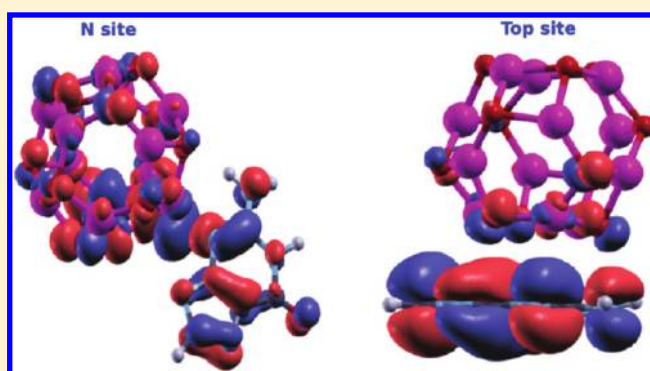
<sup>‡</sup>Department of Physics, H. P. T. Arts and R. Y. K. Science College, Nasik, Maharashtra, India

<sup>§</sup>National Physical Laboratory (NPL), Delhi, India

<sup>||</sup>U.S. Air Force Research Laboratory, Dayton, Ohio 45433, United States

<sup>⊥</sup>U.S. Army Research Laboratory, Weapons and Materials Research Directorate, ATTN: AMSRD-ARL-WM, Aberdeen Proving Ground, Maryland 20783, United States

**ABSTRACT:** We report the results of theoretical calculations on interaction of the nucleotide bases of deoxyribonucleic acid (DNA) and ribonucleic acid (RNA) with a (ZnO)<sub>12</sub> cluster, carried out within density-functional theory framework. In all cases, (ZnO)<sub>12</sub> prefers to bind with a ring nitrogen atom having a lone electron pair relative to the other possible binding sites of the bases. The degree of hybridization between Zn-d and N-p orbitals determines the relative interaction strength at the N-site of individual nucleobases with (ZnO)<sub>12</sub> in contrast to the cases of interaction of metallic clusters and carbon nanostructures with nucleobases where either electrostatic or van der Waals interactions dominates the bonding characteristics of the conjugate complexes. The predicted site-preference of (ZnO)<sub>12</sub> toward the nucleobases appears to be similar to that of the metal clusters, which indicates that the metal clusters retain their site-preference even in their oxidized state.



## 1. INTRODUCTION

Nano-bio complexes have attracted a great deal of attention in recent years due to their potential applications in such diverse fields as biomedical engineering<sup>1–3</sup> and nanoscale electronics via biotemplated self-assembly of metallic nanoparticles arrays.<sup>4–8</sup> For these novel applications, biocompatibility and interactive functionality of nanoparticles are generally required. For example, zinc oxide (ZnO) nanoparticles (NPs) have emerged themselves as a class apart due to their high degree of biocompatibility, size-tunable optical emission in the visible spectrum, and high excitonic band gap.<sup>9,10</sup> Two recent studies<sup>11,12</sup> have shown that ZnO nanoparticles can kill cancer and activated human T cells, suggesting biotherapeutic functionality of this novel material. On the other hand, a recent experimental study has shown that ZnO NPs induce significant changes in DNA structure and functionalities in the absence of photoexcitation.<sup>13</sup> Apart from these, the reason that instigates a number of rigorous and extensive studies on ZnO NPs is their sensitivity toward UV-lights,<sup>14–16</sup> which enables them to block the part of sunlight in UV-regime. It is, therefore, not surprising that ZnO NPs are an essential component of sunscreens.<sup>17,18</sup>

Despite the multifarious biomedical applications of ZnO nanoparticles, we still lack the complete understanding of the

underlying physics and chemistry involved in the ZnO–bio conjugate systems. This is due to the complexity of the macro molecules [e.g., DNA, protein] and also the fact that the functionality of biomolecules critically depends upon the site-specificity/-selectivity of the nanoparticles. The present status, therefore, requires a more detailed knowledge of the oxide–biomolecules interactions at the fundamental level. Because full scale quantum mechanical calculations consisting of DNA-strands are prohibitively expensive, we begin with the nucleobases, the building blocks of the genetic macromolecules (DNA/RNA), to look into what are the factors that might play an important role in these kinds of nano-bio interactions. Recently, there has been a keen interest in understanding the interaction between nucleobases and nanostructured materials<sup>19–28</sup> due to the potential application of the unique signature of the latter in probing the structural and conformational changes<sup>29,30</sup> of the former.

Specifically, in the present study, we have performed a first-principles quantum chemical study of the complex involving

**Received:** February 10, 2011

**Revised:** April 26, 2011

**Published:** May 10, 2011

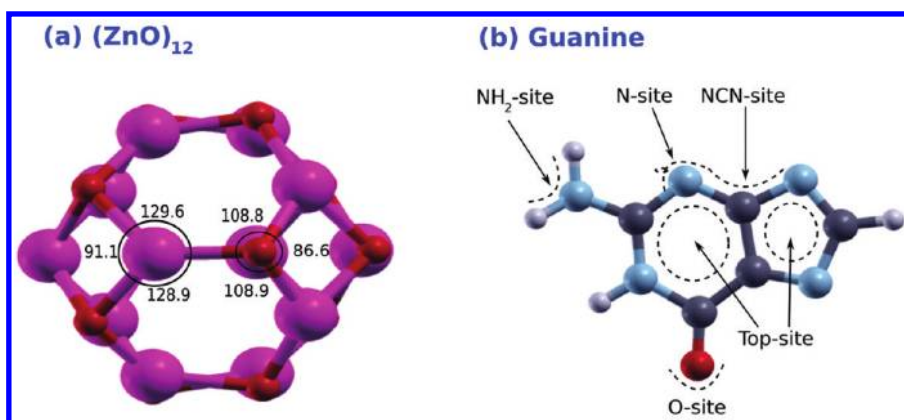


**Figure 1.** (a) The calculated ground-state configuration of  $(\text{ZnO})_{12}$ . (b) Different binding sites of guanine (Zn, magenta; C, gray; N, blue; H, grayish white; O, red).

ZnO nanoparticles and the nucleotide bases of deoxyribonucleic acid (DNA), and ribonucleic acid (RNA), adenine (A), guanine (G), cytosine (C), thymine (T), and uracil (U). The site-specificity/-selectivity of the metal oxide cluster toward the biomolecules was duly taken care of in this study. Spherical ZnO nanoparticles, represented by the cage-like small  $(\text{ZnO})_{12}$  cluster, was considered, as it has been reported to be highly symmetric and stable.<sup>31–33</sup>

## 2. COMPUTATIONAL DETAILS

Electronic structure calculations were performed in the framework of density functional theory (DFT) with the exchange-correlation functional form proposed by Perdew, Burke, and Ernzerhof (PBE)<sup>34</sup> as implemented in the SIESTA<sup>35</sup> electronic structure code. The norm-conserving pseudopotentials were constructed for each chemical species in the bioconjugated complex using the Troullier and Martins scheme.<sup>36,37</sup> The valence configurations of H ( $1s^1$ ), C ( $2s^2 2p^2$ ), N ( $2s^2 2p^3$ ), O ( $2s^2 2p^4$ ), and Zn ( $3d^{10} 4s^2$ ) were represented by double- $\zeta$  basis sets with polarization functions (DZP).<sup>38</sup> The calculations were performed with an equivalent plane wave energy cutoff energy of 3400 eV for the grid. The calculations were considered to be converged when the force on each ion was less than 0.001 eV/Å. Along with the atomic force, the total energy convergence criterion of  $10^{-5}$  eV was also used. First, the geometrical structures of the isolated nucleobases and  $(\text{ZnO})_{12}$  were optimized without symmetry constraints. Subsequently, the optimized structures were used to calculate the energy surface describing the interaction of nucleobases with  $(\text{ZnO})_{12}$ . Note that the choice of a cage-like highly symmetric small cluster to represent a spherical ZnO nanoparticle requires only modest computational resources for electronic structure calculations.

## 3. RESULTS AND DISCUSSION

The calculated ground-state configuration of  $(\text{ZnO})_{12}$  is predicted to be a cage-like structure consisting of six  $(\text{ZnO})_2$  and eight  $(\text{ZnO})_3$  rings forming a truncated octahedron in which all Zn and O vertices remain equivalent (Figure 1a). Our results are consistent with the results of previous theoretical studies.<sup>33,39</sup> Note that several other configurations including ring and tubular configurations were found to be relatively higher in energy than the predicted ground state. The calculated structural properties of  $(\text{ZnO})_{12}$ , such as the bond lengths,  $R_{(\text{Zn}-\text{O})}$  of 1.89 and 1.97 Å,

are also in good agreement with the previously reported values 1.87 and 1.97 Å, respectively.<sup>39</sup> The Zn–O bond is mainly ionic with a charge transfer from Zn to O atoms. The gap between the highest occupied molecular orbital (HOMO) and the lowest unoccupied molecular orbital (LUMO) is calculated to be 2.5 eV.

Total energy and geometrical structure of the isolated nucleobases are calculated as a prior step to the nucleobase–ZnO complex calculations. The calculated bond lengths and bond angles of the optimized equilibrium structures for nucleobases are in good agreement with earlier reported studies.<sup>40,41</sup>  $(\text{ZnO})_{12}$  is considered to approach the nucleobases toward all possible binding sites including ring nitrogen atom (i.e., the –N site), –NH<sub>2</sub> site, –NCN site, oxygen atom (i.e., O site), and hexagonal or pentagonal rings (i.e., top site) of the base molecules. These possible binding sites for guanine are shown in Figure 1b.

To calculate the binding energy of the nucleobase–cluster complex, we used the asymptotic approach where the binding energy is defined as the difference in the total energies of the conjugated system at the equilibrium configuration and when they are far apart from each other (8 Å). The equilibrium configuration is taken to be the minimum energy configuration on the energy surface of a  $(\text{ZnO})_{12}$  approaching the target binding site of a nucleobase. The paths approaching the –N, –NH<sub>2</sub>, –NCN, and O sites were constrained in the plane of the base molecule, while the path going to the top site was constrained perpendicular to the plane of the molecule (Figure 2).  $(\text{ZnO})_{12}$  is oriented in such a way that either Zn-terminated or O-terminated surface of the cluster interacts with the target binding sites of the nucleobases, and we find that the former invariably leads to a lower energy configuration. Furthermore, the conjugated complexes representing the interaction of the O-terminated surface with nucleobases are predicted to be not stable.

The calculated values of the binding energies associated with the equilibrium configurations of complexes with Zn-terminated surface of the cluster approaching toward the different binding sites of the nucleobases are given in Table 1. The binding energy of  $(\text{ZnO})_{12}$  at the ring N site for all base molecules is higher than those at other sites. It is followed by “top” site and then “O” site of the nucleobases. Both –NCN and –NH<sub>2</sub> sites are predicted to have smaller binding energies for  $(\text{ZnO})_{12}$ . Interestingly, similar site-preference was found in the previous studies on the interaction of the nucleobases with the metal clusters.<sup>42–46</sup> We may therefore conclude that the metal clusters retain their site-preference even in their oxidized state.

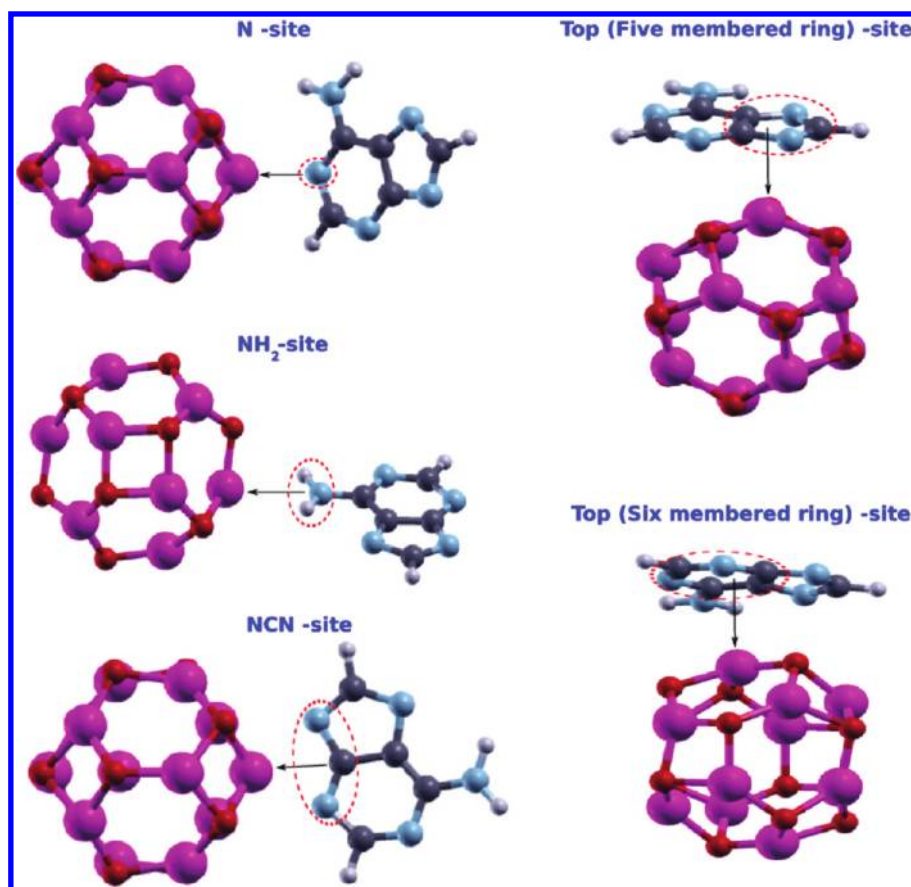


**Figure 2.** The binding sites of the adenine–(ZnO)<sub>12</sub> complex. (Zn, magenta; C, gray; N, blue; H, grayish white; O, red).

The calculated nearest-neighbor distances ( $R$ ) in the equilibrium configurations associated with the binding sites generally reflect the predicted order of the bonding energy;  $R_{Zn-N(\text{ring})}$  is in the range of 2.05–2.15 Å for the ring N site, while  $R_{Zn-C(\text{ring})}$  is about 2.5 Å for the –NCN site.  $R_{Zn-N}$  is about 3.0 Å for the least favorable –NH<sub>2</sub> site. For the top site, the nearest-neighbor distance is defined as the distance between  $Zn_{\text{cluster}}$  and the center of the five- or six-member ring of the nucleobase. It is calculated to be in the range of 2.6–2.8 Å. The calculated binding energies corresponding to the different sites thus concur with the calculated nearest-neighbor distances.

The higher binding energy found in case of N-site can be explained comparing the highest occupied molecular orbital (HOMO) of guanine–(ZnO)<sub>12</sub> complex at the N and top site equilibrium configurations [Figure 3]. The lone pair electron associated with the ring N site appears to play a key role in making it the favorable binding site for the nucleobase–(ZnO)<sub>12</sub> complex. As can be seen in Figure 3, HOMO of the ring N site configuration consists of nitrogen-p and zinc-d orbitals, whereas HOMO of the top site configuration is dominated only by  $\Pi$ -orbitals from a purine ring of guanine. It is thus the degree of hybridization of Zn-3d and N-p orbitals that leads to a greater binding energy for the ring N site relative to the top site of a nucleobase.

The order for the interaction strength for nucleobases at the preferred ring N site is as follows: C > A > U > T > G, which appears to be due to the extent of hybridization of a given base with (ZnO)<sub>12</sub>. For example, Figure 4 shows total charge densities at the N site of the cytosine–(ZnO)<sub>12</sub> and guanine–(ZnO)<sub>12</sub>

**Table 1.** Calculated Binding Energy (eV) of the Nucleobase–(ZnO)<sub>12</sub> Complex

nucleobase	–N site	–NCN site	–NH <sub>2</sub> site	top site	–O site
cytosine	1.66	–	0.17	1.22	1.02
adenine	1.48	1.06	0.18	1.32	–
uracil	1.43	–	–	1.08	0.92
thymine	1.37	–	–	1.04	0.96
guanine	1.34	1.12	0.15	1.06	0.90

complexes. The charge density is projected along (100) plane, and a superimposed ball and stick model identifies the atoms in the complex. Interestingly, the charge density plot shows a relatively large overlap of the electron density along the  $Zn_{\text{cluster}}-N_{\text{ring}}$  bond in cytosine–(ZnO)<sub>12</sub> as compared to that in the guanine–(ZnO)<sub>12</sub> complex. Thus, the relatively high binding energy (Table 1) of cytosine with (ZnO)<sub>12</sub> may be attributed to a larger degree of hybridization of Zn-3d and N-p orbitals at the ring N site in the complex. This is also confirmed by the calculated total and projected density of states (not shown here) of the complexes. It may, therefore, be concluded that the covalent forces play the key role in deciding the strength of interaction. The nearest-neighbor distance also reconfirms the interaction regime for covalent forces.<sup>47</sup> We also carried out the Mulliken population analysis to look into the contribution from the ionic forces and found an insignificant amount of charge ( $\sim 0.1e$ ) gets transferred from N to Zn at the ring N site in the equilibrium configuration



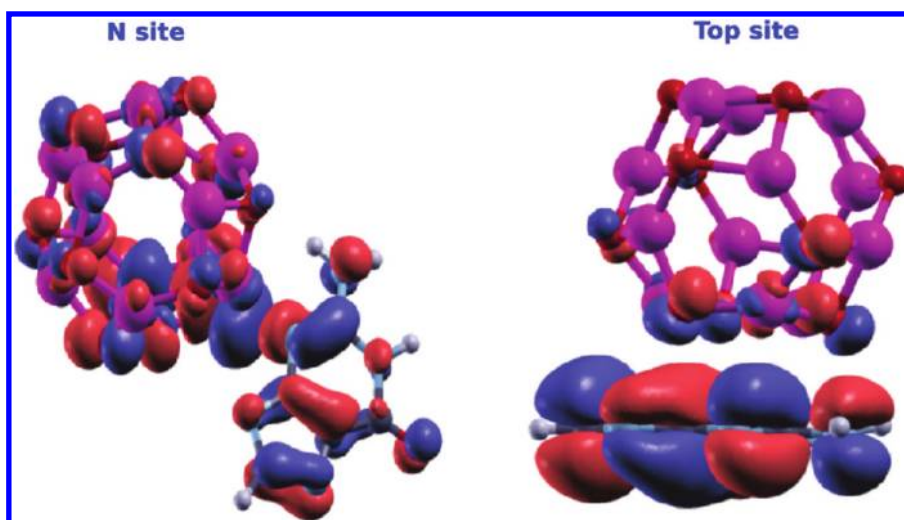


**Figure 3.** HOMO of  $(\text{ZnO})_{12}$  conjugated guanine (with N site and top site) in the equilibrium configuration. One-fifth of the maximum isosurface value was taken in both cases. (Zn, magenta; C, gray; N, blue; H, grayish white; O, red).

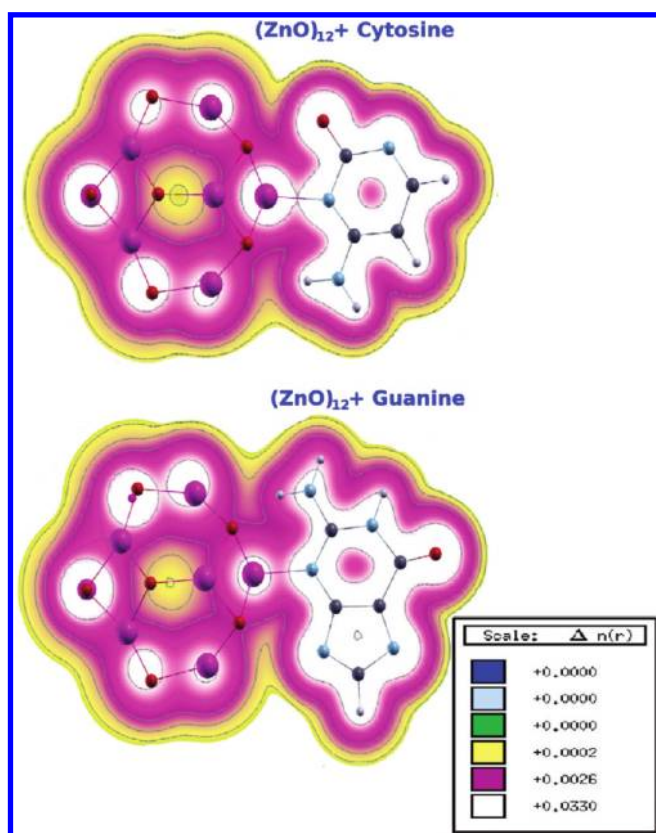


**Figure 4.** Total charge density contour plots of  $(\text{ZnO})_{12}$ +cytosine and  $(\text{ZnO})_{12}$ +guanine complexes interacting at the ring N site. The charge density is projected along the (100) plane, and a superimposed ball and stick model identifies the atoms in the complex. (Zn, magenta; C, gray; N, blue; H, grayish white; O, red).

of the complexes considered. It definitely rules out the possibility of the dominance of the Coulombic forces deciding the strength of interaction. This is not surprising if we look at the optimum distance between the cluster to the nucleobases.

A comparison of our results on ZnO with those on metallic clusters studies including Ag and Au<sup>42–46</sup> reveals that even though the site-preference is similar in both cases, the binding energy of nucleobases with  $(\text{ZnO})_{12}$  at the N site is significantly higher than that of metallic Ag and Au clusters–nucleobase complexes. This may be due to a difference in the bonding characteristics of metal–nucleobase and ZnO–nucleobase complexes. A considerable charge transfer from nucleobases to metallic cluster is calculated, suggesting the dominance of electrostatic interactions in the metal–nucleobase conjugates. On the other hand, covalent interactions via the degree of mixing of electronic states appear to dominate the interaction between  $(\text{ZnO})_{12}$  and nucleobases.

Previously, the physisorption of the nucleobases on a planar sheet graphene,<sup>23</sup> on small diameter carbon nanotubes (CNTs),<sup>24</sup> and on boron nitride nanotubes (BNNTs)<sup>48</sup> was investigated where the interactions between graphene and CNTs with nucleobases are also dominated by vdW forces. However, the semiconducting BNNTs interacting with nucleobases show that the interaction not only depends upon their individual polarizability leading to vdW interactions but also marginally depends on the degrees of mixing of electronic states with the tubular surface of the BNNT. ZnO cluster, being semiconducting in nature, qualitatively resembles BNNT as far as the nature of forces that comes into consideration while interacting with the nucleobases.

#### 4. CONCLUSIONS

We have investigated the interaction of  $(\text{ZnO})_{12}$  with the nucleic acid bases, adenine, guanine, cytosine, thymine, and uracil, in the framework of density functional theory. The interaction strength expressed in terms of the binding energy is found to be highest at the ring nitrogen site for all nucleobases, the sequence being  $G < T < U < A < C$ . The interaction between the ZnO-cluster and nucleobases is dominated by the covalent and weak vdW forces, where the degree of hybridization between Zn-d with N-p orbitals determines the relative interaction strength of individual nucleobases and  $(\text{ZnO})_{12}$  with a marginal contribution from the ionic forces. The results of the present study constitute a preliminary step toward understanding the

observed damage of the structural configuration of DNA by ZnO nanoparticles. Work is in progress to calculate interaction of single-stranded DNA with ZnO nanoparticles and also to look into how the nucleobases retain their site-preference when the actual DNA is in aqueous media. The work will also be extended to study zinc nanostructures, for example, functionalized ZnO tetrapods,<sup>49</sup> which can be used as carriers for mammalian cell transfections.

## AUTHOR INFORMATION

### Corresponding Author

\*E-mail: pandey@mtu.edu (R.P.); shashi.karna@us.army.mil (S.P.K.).

## ACKNOWLEDGMENT

We gratefully acknowledge V. Shanker and S. Gowtham for their constructive criticism and fruitful scientific discussions. V.S. and P.J. also acknowledge Michigan Technological University for providing local hospitality. M.D. and V.S. acknowledge the financial assistance from the Department of Science and Technology (DST), Government of India. R.P. acknowledges the financial support of the Henry M. Jackson Foundation for the Advancement of Military Medicine, Inc.

## REFERENCES

- (1) Nagasaki, Y. *Chem. Lett.* **2008**, *37*, 564–569.
- (2) Huang, X.; El-Sayed, I. H.; Qian, W.; El-Sayed, M. A. *Nano Lett.* **2007**, *7*, 1591–1597.
- (3) Oberdorster, G.; Oberdorster, E.; Oberdorster, J. *Environ. Health Perspect.* **2005**, *113*, 823–839.
- (4) Whaley, S. R.; English, D. S.; Hu, E. L.; Barbara, P. F.; Belcher, A. M. *Nature* **2000**, *405*, 665–668.
- (5) Le, J. D.; Pinto, Y.; Seeman, N. C.; Musier-Forsyth, K.; Talon, T. A.; Kiehl, R. A. *Nano Lett.* **2004**, *4*, 2343–2347.
- (6) Pinto, Y. Y.; Le, J. D.; Seeman, N. C.; Musier-Forsyth, K.; Taton, T. A.; Kiehl, R. *Nano Lett.* **2005**, *5*, 2399–2400.
- (7) Zheng, J.; Constantinou, P. E.; Micheel, C.; Alivisatos, A. P.; Kiehl, R. A.; Seeman, N. C. *Nano Lett.* **2006**, *6*, 1502–1504.
- (8) Sharma, J.; Chhabra, R.; Liu, Y.; Ke, Y. G.; Yan, H. *Angew. Chem., Int. Ed.* **2006**, *45*, 730–735.
- (9) Wu, Y. L.; Lim, C. S.; Fu, S.; Tok, A. I. Y.; Lau, H. M.; Boey, F. Y. C.; Zeng, X. T. *Nanotechnology* **2007**, *18*, 215604–1–9.
- (10) Wu, Y. L.; Fu, S.; Tok, A. I. K.; Zeng, X. T.; Lim, C. S.; Kwek, L. C.; Boey, F. Y. C. *Nanotechnology* **2008**, *19*, 345605–1–9.
- (11) Hanley, C.; Layne, J.; Punnoose, A.; Reddy, K. M.; Coombs, I.; Coombs, A.; Feris, K.; Wingett, D. *Nanotechnology* **2008**, *19*, 295103–1–10.
- (12) Reddy, K. M.; Feris, K.; Bell, J.; Wingett, D. G.; Hanley, C.; Punnoose, A. *Appl. Phys. Lett.* **2007**, *90*, 213902–1–3.
- (13) Sharma, V.; Shukla, R. K.; Saxena, N.; Parmar, D.; Das, M.; Dhawan, A. *Toxicol. Lett.* **2009**, *185*, 211–218.
- (14) Soci, S.; Zhang, A.; Xiang, B.; Dayeh, S. A.; Aplin, D. P. R.; Park, J.; Bao, X. Y.; Lo, Y. H.; Wang, D. *Nano Lett.* **2007**, *7*, 1003–1009.
- (15) Bera, A.; Basak, D. *Appl. Phys. Lett.* **2008**, *93*, 053102–1–3.
- (16) Liu, K. W.; Shen, D. Z.; Shan, C. X.; Zhang, J. Y.; Yao, B.; Zhao, D. X.; Lu, Y. M.; Fan, X. W. *Appl. Phys. Lett.* **2007**, *91*, 201106–1–3.
- (17) Thomas, T.; Thomas, K.; Sadrieh, N.; Savage, N.; Adair, P.; Bronaugh, R. *Toxicol. Sci.* **2006**, *91*, 14–19.
- (18) Musarrat, J.; Saquib, Q.; Azam, A.; Naqvi, S. A. H. *Int. J. Nanopart.* **2009**, *2*, 402–415.
- (19) Ortmann, F.; Schmidt, W. G.; Bechstedt, F. *Phys. Rev. Lett.* **2005**, *95*, 186101–1–4.
- (20) Jeng, E. S.; Moll, A. E.; Roy, A. C.; Gastala, J. B.; Strano, M. S. *Nano Lett.* **2006**, *6*, 371–375.
- (21) Meng, S.; Maragakis, P.; Papaloukas, C.; Kaxiras, E. *Nano Lett.* **2007**, *7*, 45–50.
- (22) Enyashin, A. N.; Gemming, S.; Seifert, G. *Nanotechnology* **2007**, *18*, 245702–1–10.
- (23) Gowtham, S.; Scheicher, R. H.; Ahuja, R.; Pandey, R.; Karna, S. P. *Phys. Rev. B* **2007**, *76*, 033401–1–4.
- (24) Gowtham, S.; Scheicher, R. H.; Pandey, R.; Karna, S. P.; Ahuja, R. *Nanotechnology* **2008**, *19*, 125701–1–6.
- (25) Johnson, R. R.; Johnson, A. T. C.; Klein, M. L. *Nano Lett.* **2008**, *8*, 69–75.
- (26) Das, A.; Sood, A. K.; Maiti, P. K.; Das, M.; Varadarajan, R.; Rao, C. N. R. *Chem. Phys. Lett.* **2008**, *453*, 266–273.
- (27) Johnson, R. R.; Kohlmeyer, A.; Johnson, A. T. C.; Klein, M. L. *Nano Lett.* **2009**, *9*, 537–541.
- (28) Tu, X. M.; Manohar, S.; Jagota, A.; Zheng, M. *Nature* **2009**, *460*, 250–253.
- (29) Vaidyanathan, V. G.; Nair, B. U. *J. Inorg. Biochem.* **2003**, *95*, 334–342.
- (30) Rajendran, A.; Magesh, C. J.; Perumal, P. T. *Biochim. Biophys. Acta* **2008**, *1780*, 282–288.
- (31) Dmytruk, A.; Dmitruk, I.; Blonskyy, I.; Belosludov, R.; Kawazoe, Y.; Kasuya, A. *Microelectron. J.* **2009**, *40*, 218–220.
- (32) Wang, B.; Wang, X.; Chen, G.; Nagase, S.; Zhao, J. *J. Chem. Phys.* **2008**, *128*, 144710–1–6.
- (33) Zhao, M.; Xia, Y.; Tan, Z.; Liu, X.; Mei, L. *Phys. Lett. A* **2007**, *372*, 39–43.
- (34) Perdew, J. P.; Burke, K.; Ernzerhof, M. *Phys. Rev. Lett.* **1996**, *77*, 3865–3868.
- (35) Soler, J. M.; Artacho, E.; Gale, J. D.; García, A.; Junquera, J.; Ordejón, P.; Sánchez-Portal, D. *J. Phys.: Condens. Matter* **2002**, *14*, 2745–2779.
- (36) Troullier, N.; Martins, J. L. *Phys. Rev. B* **1991**, *43*, 1993–2006.
- (37) Kleinman, L.; Bylander, D. M. *Phys. Rev. Lett.* **1982**, *48*, 1425–1428.
- (38) Sanchez-Portal, D.; Artacho, E.; Soler, J. M. *J. Phys.: Condens. Matter* **1996**, *8*, 3859–3880.
- (39) Wang, B.; Nagase, S.; Zhao, J.; Wang, G. *J. Phys. Chem. C* **2007**, *111*, 4956–4963.
- (40) Espejo, C.; Rey-González, R. R. *Rev. Mex. Fis. S* **2007**, *53*, 212–216.
- (41) Sponer, J.; Hobza, P. *J. Phys. Chem.* **1994**, *98*, 3161–3164.
- (42) Soto-Verdugo, V.; Metiu, H.; Gwinn, E. *J. Chem. Phys.* **2010**, *132*, 195102–1–10.
- (43) Kryachko, E. S.; Remacle, F. *J. Phys. Chem. B* **2005**, *109*, 22746–22757.
- (44) Kumar, A.; Mishra, P. C.; Suhai, S. *J. Phys. Chem. A* **2006**, *110*, 7719–7727.
- (45) Sharma, P.; Singh, H.; Sharma, S.; Singh, H. *J. Chem. Theory Comput.* **2007**, *3*, 2301–2311.
- (46) Shukla, M. K.; Dubey, M.; Zakar, E.; Leszczynski, J. *J. Phys. Chem. C* **2009**, *113*, 3960–3966.
- (47) Grabowski, S. J.; Sokalski, W. A.; Dyguda, E.; Leszczynski, J. *J. Phys. Chem. B* **2006**, *110*, 6444–6446.
- (48) Mukhopadhyay, S.; Gowtham, S.; Scheicher, R. H.; Pandey, R.; Karna, S. P. *Nanotechnology* **2010**, *21*, 165703–1–6.
- (49) Nie, L.; Gao, L.; Yan, X.; Wang, T. *Nanotechnology* **2007**, *18*, 015101–1–6.